AGU PUBLICATIONS

Geophysical Research Letters

RESEARCH LETTER
10.1002/2017GL073632

Key Points:
- Last Glacial Maximum (21 ka B.P.) ice sheets drive weakening of the North American Monsoon by altering the large-scale atmospheric flow
- Cooling resulting from high ice sheet albedo weakens the monsoon flow and favors the import of cold, dry air into the monsoon region
- Modeled glacial response of the North American Monsoon is primarily driven by the atmospheric circulation rather than oceanic changes

Supporting Information:
- Supporting Information S1
- Figure S1
- Figure S2
- Figure S3
- Figure S4
- Figure S5

Correspondence to:
T. Bhattacharya,
tripti@email.arizona.edu

Citation:
Bhattacharya, T., J. E. Tierney, and P. DiNezio (2017), Glacial reduction of the North American Monsoon via surface cooling and atmospheric ventilation, *Geophys. Res. Lett.*, *44*, 5113–5122, doi:10.1002/2017GL073632.

Received 28 MAR 2017
Accepted 8 MAY 2017
Accepted article online 11 MAY 2017
Published online 27 MAY 2017

Glacial reduction of the North American Monsoon via surface cooling and atmospheric ventilation

Tripti Bhattacharya[1], **Jessica E. Tierney**[1], **and Pedro DiNezio**[2]

[1]Department of Geosciences, University of Arizona, Tucson, Arizona, USA, [2]Institute for Geophysics, University of Texas at Austin, Austin, Texas, USA

Abstract The North American Monsoon (NAM) provides critical water resources to the U.S. southwest and northwestern Mexico. Despite its importance to regional hydrology, the mechanisms that shape this monsoon are not fully understood. In this paper, we use model simulations of the Last Glacial Maximum (LGM, 21 ka B.P.) to assess the sensitivity of the NAM to glacial boundary conditions and shed light on its fundamental dynamics. We find that atmospheric changes induced by ice sheet albedo reduce NAM intensity at the LGM. The high albedo of the Laurentide ice sheet cools the surface and drives anomalous northwesterly winds that reduce the monsoon circulation and import cold, dry air into the core NAM region. Our work emphasizes the role of ice sheet albedo rather than topography in driving the atmospheric changes that modulate the glacial NAM, and ties our understanding of the NAM to broader theories of monsoon systems.

1. Introduction

In the arid U.S. southwest and northwest Mexico, the North America Monsoon (NAM) provides critical water resources for a growing human population and sustains unique, biodiverse ecosystems [*Ray et al.*, 2007; *Turner et al.*, 1995]. Despite the NAM's critical importance in regional hydrology, its seasonal evolution and long-term variability is not fully understood. For instance, the NAM features shallower summertime convection and low-level wind reversals than other canonical monsoons [*Nie et al.*, 2010; *Bordoni and Stevens*, 2006]. *Mitchell et al.* [2002] established the role of Gulf of California (GoC) sea surface temperatures (SSTs) in driving the northward propagation of monsoon convection, leading *Barron et al.* [2012] to suggest that the NAM tracks GoC temperatures on millennial time scales. Current debates about the NAM focus on the relative importance of remote and local moisture sources to the monsoon and the impact of the large-scale atmospheric flow [*Schiffer and Nesbitt*, 2012; *Chou and Neelin*, 2003]. More detailed knowledge of NAM dynamics can improve our ability to predict the NAM's response to rising greenhouse gases, especially given that global and regional models generate divergent predictions of NAM behavior under global warming [*Cook and Seager*, 2013; *Meyer and Jin*, 2016].

To better understand the sensitivity of the NAM to global climatic changes, we analyze NAM changes associated with the Last Glacial Maximum (LGM, 21 ka B.P.). The LGM represented a dramatic departure from preindustrial boundary conditions, with extensive continental ice sheets, lowered sea level, and reduced greenhouse gases [*Braconnot et al.*, 2012]. The pronounced changes in Earth's climate at the LGM offer a natural experiment for evaluating different theories about the NAM, including its sensitivity to changes in SSTs on paleoclimatic time scales. Investigation of the NAM during the LGM from a modeling perspective may also aid paleoclimatic interpretations.

Paleoclimate proxy data suggest an overall wetter LGM in the NAM region due to shifts in the westerly winds and increases in wintertime precipitation [*Wagner et al.*, 2010; *Asmerom et al.*, 2010; *Railsback et al.*, 2015; *Caballero-Miranda*, 1997; *Oster et al.*, 2015]. NAM changes are less clear as they are generally masked by the magnitude of the winter signal. Geomorphic and lacustrine records from the American Southwest imply that the NAM was weaker prior to the Holocene [*Roy et al.*, 2015; *Antinao and McDonald*, 2013], but a speleothem from southern Mexico suggests that the LGM NAM was as strong as present day [*Lachniet et al.*, 2013].

Dynamic explanations for glacial NAM changes are similarly diverse. Some researchers posit that SSTs in the GoC were too cold to support a monsoonal circulation during the LGM [*Barron et al.*, 2012; *Metcalfe et al.*, 2015].

Monsoon changes have also been linked to the position of the Intertropical Convergence Zone (ITCZ) [*Lachniet et al.*, 2013; *Jiang et al.*, 2015]. Alternatively, the LGM NAM may have been entirely suppressed by the westerlies [*Thompson and Anderson*, 2000].

Here we use a suite of simulations using the model Community Earth System Model v.1.2 (CESM1.2) to investigate the changes in the NAM during the LGM and the processes responsible for driving these changes. While revealing unique aspects of the NAM circulation under glacial boundary conditions, this work also links our understanding of the NAM to broader theories of monsoon dynamics [*Privé and Plumb*, 2007], with important implications for understanding its present climatology and future behavior.

2. Data and Methods

Simulations were performed using the Community Earth System Model v.1.2 (CESM1.2), the most recent general circulation model (GCM) developed by the National Center for Atmospheric Research (NCAR). The atmospheric component is the Community Atmosphere Model version 5 (CAM5) [*Neale et al.*, 2010]. Land and ocean components are described in *Lawrence et al.* [2011] and *Smith et al.* [2010]. Atmospheric and land models were run at a 2° resolution with prescribed vegetation cover, while the ocean model was run at a nominal 1° resolution. Following *Cook and Seager* [2013], we define the NAM region as the land area between 18° and 33°N and 112° – 102°W and use this area to define averages of the NAM circulation.

We applied the LGM boundary conditions defined in the Paleoclimate Model Intercomparison Project 3's (PMIP3) experimental protocols to the fully coupled CESM1.2 model (FullLGM) (see https://wiki.lsce.ipsl.fr/pmip3/doku.php/pmip3:design:21k:final). We subtracted this simulation from the fully coupled run forced with preindustrial boundary conditions (PIControl) to identify LGM anomalies. Statistical significance was calculated using a Student's *t* test.

Climatological plots suggest that CESM simulates a reasonable summertime North American Monsoon as compared to data from the Global Precipitation Climatology Centre (GPCC) [*Schneider et al.*, 2014]. The modeled monsoon peaks later than observations, but it captures the correct magnitude of the seasonal changes in rainfall (supporting information Figure S1). While we recognize that some processes associated with the NAM may not be well represented in coarser-resolution GCMs generally [*Meyer and Jin*, 2016], CESM is an appropriate tool for assessing large-scale changes in response to glacial boundary conditions. Furthermore, other models in the PMIP3 archive produce essentially the same pattern of LGM NAM change as seen in CESM, improving confidence in our particular choice of GCM (Figure S2). We choose to focus our analysis on July – September rainfall, since this is the monsoon peak in the modern observational climatology and the period with the strongest, statistically significant LGM anomalies (Figures 1 and S1). Details on model equilibration times and run lengths are provided in the supporting information.

Additional experiments were configured using different combinations of preindustrial and LGM boundary conditions in a series of "single-forcing" simulations. To identify the influence of an individual boundary condition on the NAM, we performed an experiment setting only that boundary condition to LGM values. For instance, the greenhouse gas simulation (GhGOnly) was configured with preindustrial boundary conditions except for LGM greenhouse gas concentrations. Similarly, the ice sheet (IceSheetOnly) and ice sheet topography (IceSheetNoAlbedo) simulations isolated the climatic influence of LGM ice sheets and ice sheet topography, respectively. IceSheetNoAlbedo included the topography of the ice sheet with surface albedo set to preindustrial values. This results in a low albedo "brown ice sheet" during the summer with higher albedo in winter as snow cover develops over part of the ice sheet in accordance with preindustrial climatology.

We also isolated the atmospheric response to the presence of ice sheets in an atmosphere-only simulation where the ocean model is replaced with seasonally varying SSTs from the fully coupled preindustrial control run. This uncoupled simulation (IceSheetAtm) was contrasted with a similar atmosphere-only simulation with preindustrial boundary conditions (PIAtm). The influence of atmosphere-ocean interactions was determined in an additional simulation that coupled CAM5 to a "slab ocean" in which SSTs were only influenced by atmospheric energy exchanges (IceSheetSlab). Subtracting IceSheetSlab from IceSheetAtm helped isolate the influence of SST changes that result from atmosphere-ocean energy exchanges. Details of these simulations are given in Table 1.

We used fields of precipitation, evaporation, temperature, meridional and zonal winds, vertical velocity, geopotential height, and specific humidity to diagnose the causes of rainfall changes. To identify changes in

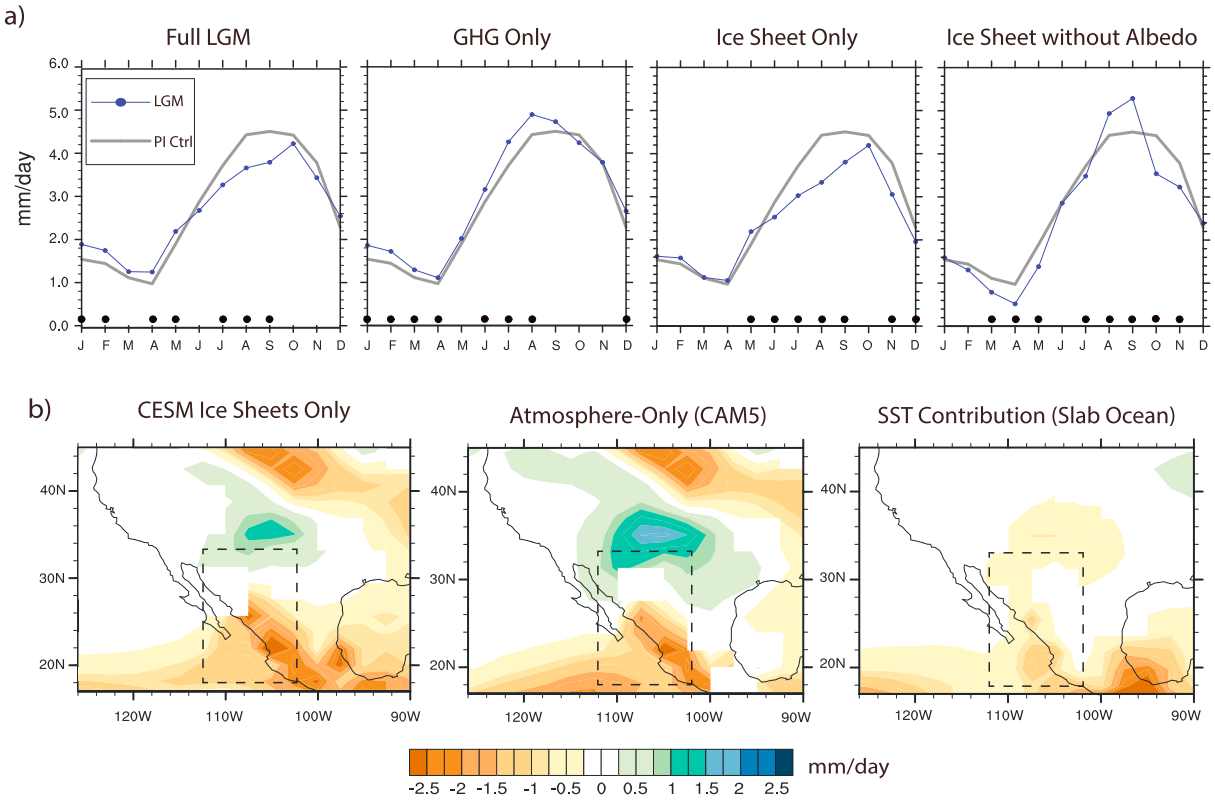

Figure 1. (a) Single-forcing runs of CESM1.2, varying individual forcings at the LGM. Modern climatology is shown in gray, while LGM anomalies are shown in blue. (b) Comparison of rainfall anomalies in Ice Sheet Only simulations for JAS, showing the fully coupled simulation (IceSheetOnly), Atmosphere-Only response to ice sheet (IceSheetAtm), and the additional contribution of the slab ocean (IceSheetSlab−IceSheetAtm). The boxes outline the area used to define climatologies for the NAM, only land areas are included in spatial averages. Statistical significance is calculated using a Student's *t* test. In Figure 1a, black circles on *x* axis indicate that monthly anomalies are statistically significant at the 99% level. In Figure 1b, only grid cells that are significant at 99% are shown.

the energy available for NAM convection, we calculated moist static energy (MSE), which is a measure of the energy within a parcel of air, integrating information from the geopotential (parcel's height z multiplied by the gravitational constant g), temperature (T multiplied by the specific heat C_p), and moisture content (specific humidity q multiplied by the latent heat of vaporization L_v) [see *Holton and Hakim*, 2012]:

$$MSE = C_p \cdot T + L_v \cdot q + g \cdot z \tag{1}$$

We also calculated the advection of MSE, using mean fields to diagnose the contribution from anomalous winds versus changes in the MSE gradient:

$$(V \cdot \nabla MSE)' = V' \cdot \nabla MSE_{\text{clim}} + V_{\text{clim}} \cdot (\nabla MSE)' \tag{2}$$

This ignores the contribution of eddies, which likely play an important role in energy diffusion in the glacial atmosphere. However, equation (2) provides a useful estimate of the contribution of advection by changes in the mean flow to energetic changes in the NAM region. Climatological values are taken from the PIControl simulation, while $'$ symbols represent LGM deviations from preindustrial climatology. Fields of MSE and advection are vertically integrated from the surface to the top of the atmosphere. Other studies have used similar, MSE-based approaches to analyze rainfall changes [*Chou et al.*, 2009; *Cook and Seager*, 2013].

3. Results and Discussion

3.1. Primacy of Ice Sheet Influence

CESM1.2 simulates strong reductions in July–September (JAS) NAM rainfall in the fully coupled LGM simulation (Figure 1). The largest rainfall reductions in the NAM region occur between 30 and 20°N, in the core of

Table 1. Simulations of CESM1.2 Using Different Configurations of Last Glacial Maximum (LGM) Boundary Conditions

Simulation ID	Description	Response Isolated	Calculation Method
PIControl	Preindustrial (1850 AD) greenhouse gas concentrations, land cover, bathymetry, and orbital conditions, fully coupled	n/a	n/a
PIAtm	Same as PI Control but only run with CAM5 coupled to fixed present-day SSTs	n/a	n/a
PISlab	Same as PI Control but with CAM5 coupled to a slab ocean of 200 m depth	n/a	n/a
FullLGM	Fully coupled CESM1.2 run with full LGM boundary conditions	Full LGM	FullLGM – PIControl
GhGOnly	Present-day conditions with LGM greenhouse gas concentrations, based on PMIP3 experimental protocol	Greenhouse gases	GhGOnly–PIControl
IceSheetOnly	Present-day conditions with LGM continental ice sheets (based on PMIP3)	Ice sheets	IceSheetOnly–PIControl
IceSheetAtm	Ice Sheet Only with fixed present day SSTs coupled to CAM5	Atmospheric response to ice sheet	IceSheetAtm–PIAtm
IceSheetSlab	Ice Sheet Only with 200 m slab ocean coupled to CAM5	Mixed layer response to ice sheets	IceSheetSlab–IceSheetAtm
IceSheetNoAlbedo	Ice Sheet with brown surface	Ice sheet topography	IceSheetnoAlbedo–PIControl and IceSheetOnly–IceSheetNoAlbedo

the NAM region. The northernmost part of the NAM region experiences increased rainfall, resulting from a southward shift of a stationary wave pattern in the westerlies, evident in the southwesterly wind anomalies at 30°N in Figure 2. Rainfall changes in the northern NAM region are smaller than the anomalies farther south, resulting in overall negative rainfall anomalies in the NAM region (Figure 1).

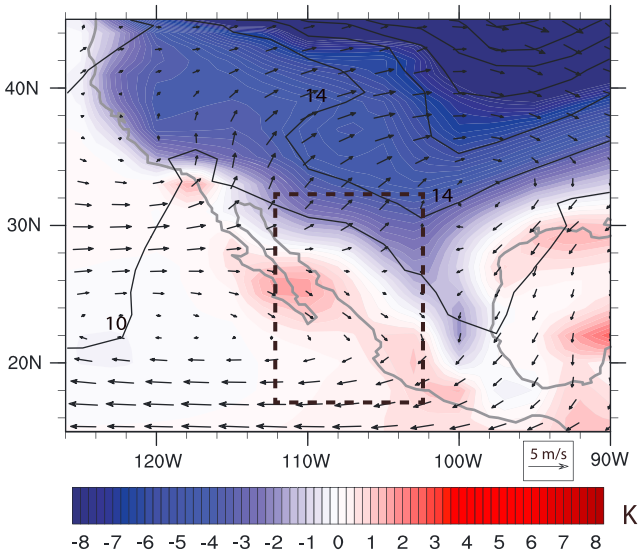

Figure 2. July–September anomalies of low-level temperature (shaded contours, K), surface pressure (solid contours, Pa), and 850 hPa winds (vectors, m/s) from the CAM5 simulation with Ice Sheets (IceSheetAtm). Changes in the pressure field strongly conform to temperature changes and drive northwesterly anomalies in the NAM region, indicating weakening of the monsoon flow. The box outlines the area used to define climatologies for the NAM; only land areas are included in spatial averages.

Single-forcing simulations show that ice sheet albedo is the critical factor in causing NAM reductions at the LGM. LGM changes in greenhouse gases (GHGOnly) have little influence on JAS rainfall in the NAM region, and the simulation with present-day albedo on ice sheet topography (IceSheetNoAlbedo) actually increases JAS rainfall (Figure 1). Only the simulation including ice sheet topography and albedo (IceSheetOnly) produces a reduction in NAM rainfall (Figure 1a).

Our analyses suggest that the atmosphere is key in communicating the influence of ice sheet albedo to the NAM region. Figure 1b shows that the pattern of negative rainfall anomalies in the fully coupled run (IceSheetOnly) is also present in the atmosphere-only run with ice sheets (IceSheetAtm). The atmosphere alone is

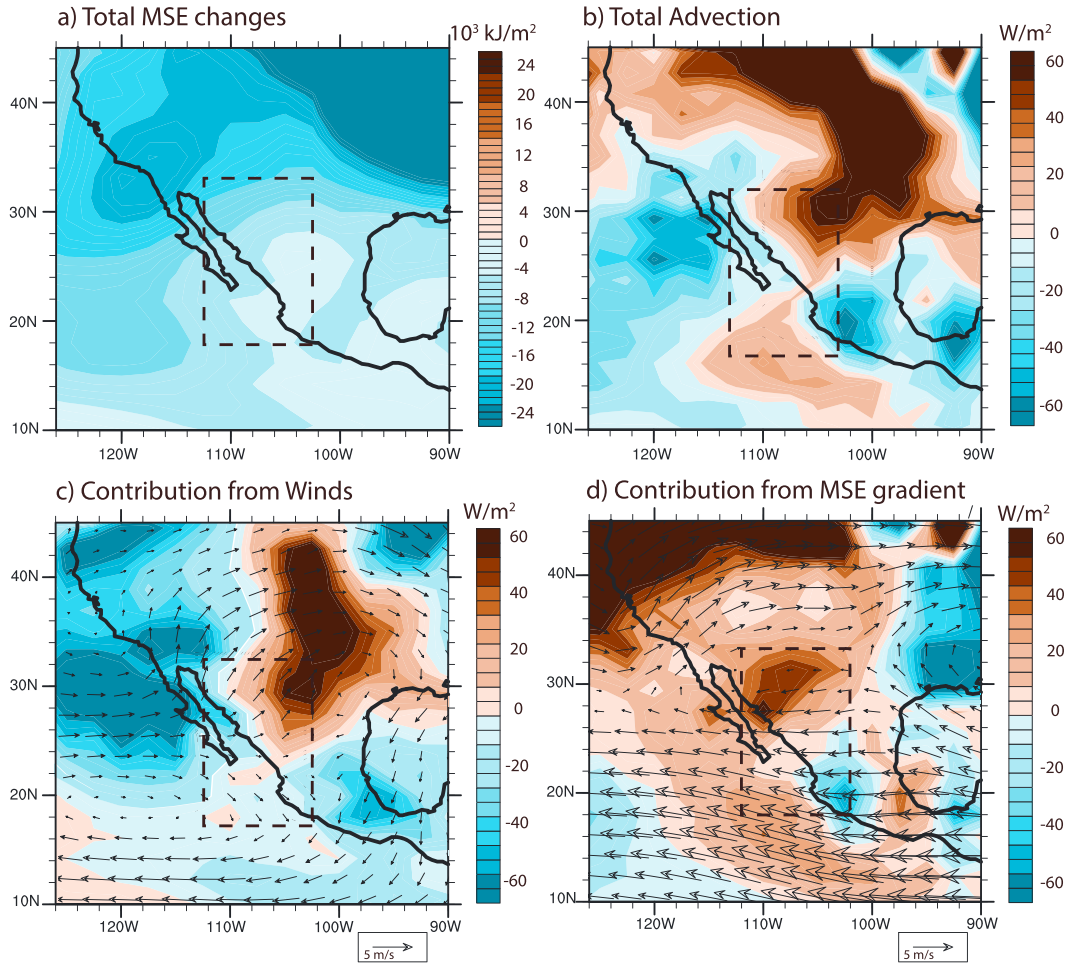

Figure 3. Anomalous advection of moist static energy (MSE) integrated over the atmospheric column for JAS. (a) Total column MSE changes. For reference, the boxes outline the area used to define climatologies for the NAM. (b) Total MSE advection by the mean flow; (c) contribution from anomalous winds and the climatological gradient of MSE, with 850 hPa JAS wind anomalies (vectors). (d) Contribution from the altered gradient of MSE and climatological JAS winds (vectors).

able to produce a 2 mm/day rainfall reduction in the NAM region (Figure 1). In contrast, the presence of a slab ocean (calculated as IceSheetSlab−IceSheetAtm) only reduces monsoon rainfall by an additional 0.5 mm/day in the NAM domain, smaller in magnitude than the direct atmospheric contribution (Figure 1). This reduction likely results from SST cooling in response to ice sheet-induced surface energy budget changes [*Manabe and Broccoli*, 1985].

3.2. Atmospheric Dynamics and Ventilation

Several mechanisms contribute to NAM weakening in response to high ice sheet albedo. High albedo reflects shortwave radiation, cooling the land surface (Figure S3). This cooling increases surface pressure and reduces the onshore pressure gradient necessary to drive monsoon winds, resulting in a weakening of the NAM circulation (Figure 2). This is evidenced by anomalous northwesterly winds across the core NAM region in response to LGM boundary conditions (Figure 2). To the north of the NAM region, southwesterly winds are the result of an enhanced meridional temperature gradient and southward shift in the westerlies and a stationary wave pattern (Figure 2).

The anomalous atmospheric flow also reduces the energy available for NAM convection by increasing advection of low-MSE air. Figure 3 shows changes in total MSE, as well as MSE advection for the atmosphere-only model forced with ice sheets (IceSheetAtm). Nearly identical results are produced by the full LGM fully coupled CESM simulation (Figure S4). The atmosphere's response to the ice sheet reduces MSE across the entire NAM region (Figure 3a). Much of this change is due to advection by changes in the mean flow, especially near

20°N (Figure 3b). The total change in advection is largely determined by changes in winds, which create northwesterly anomalies along the west coast of Mexico (Figure 3c). Changes in the MSE gradient contribute slightly to energy reductions in the southern part of the domain but generally favor the import of high-energy air (Figure 3d). Advection by the mean flow does not account for total MSE changes (Figure 3a). Our advection calculation neglects the effect of eddies, and given the sharp meridional gradients of MSE and temperature over North America (Figures 3b and 2), eddies would diffuse low-MSE air southward, further enhancing monsoon ventilation. Enhanced baroclinic instability due to strong meridional temperature gradients and a southward shift in the westerlies would increase transient eddy activity at the LGM, further increasing ventilation (Figure S5).

Ice sheet-induced changes in atmospheric circulation drive the majority of the NAM rainfall reduction in response to ice sheets, with a secondary contribution from the SST cooling (Figure 1). In particular, climatological changes to the wind field induce the import of cold, dry air into coastal regions of the NAM domain (Figure 3), a process that would be enhanced by eddies (Figure S5). This process is known to limit the northward extent of monsoons and is called "ventilation," defined by *Chou and Neelin* [2003] as the advection of low-MSE air into monsoon regions or export of high MSE air out of monsoon regions.

Our finding that ventilation plays a strong role in regulating the NAM under LGM boundary conditions emphasizes the importance of midlatitude circulations in regulating monsoon dynamics. *Chou and Neelin* [2003] note that in tropical settings surface fluxes of sensible and latent heat may be sufficient to drive a monsoon. In contrast, in midlatitude regimes, the transport of energy by the circulation may play an important role in the local energy budget and could potentially modulate the strength of monsoon circulations [*Chou and Neelin*, 2003]. Support for this latter interpretation comes from previous studies that turned off ventilation, prescribed cooling, or eliminated mountain ranges and showed that the intrusion of low-MSE air masses into monsoon regions weakens the circulation and limits the northward extent of convection [*Chou and Neelin*, 2003; *Boos and Kuang*, 2010; *Hurley and Boos*, 2013; *Liu et al.*, 2014].

3.3. Ice Sheet Albedo and Westerly Wind Changes

Our single-forcing experiments reveal that changes in ice sheet albedo are essential drivers for weakening the NAM (Figure 1). A key aspect of the circulation change in the IceSheetAtm run involves a southward shift in the westerly winds, which are strongly linked to the cooling influence of the ice sheet. The inclusion of high albedo values over the ice sheet alters the surface energy budget and substantially cools North America, resulting in strong meridional gradients of 500 hPa temperature and geopotential heights (Figure 4). These gradients enhance westerly winds south of the ice sheet since we expect the largest zonal wind anomalies to be colocated with the strongest meridional temperature and geopotential height gradients [*Holton and Hakim*, 2012]. The cooling influence of ice sheet albedo is therefore necessary to drive westerly wind anomalies far south of the ice sheet and create northwesterly anomalies over the NAM region.

Our results contrast with previous work that emphasizes the role of ice sheet topography in LGM climate [*Lee et al.*, 2015; *Pausata et al.*, 2011], this apparent contradiction can be resolved by considering seasonality. Previous work primarily focused on the winter response of the circulation to ice sheets. Given that much of the region covered by the Laurentide Ice Sheet is covered in snow in the winter months, even our IceSheetNoAlbedo simulation would produce a similar response to the full ice sheet simulation (IceSheetOnly) during winter. In summer, however, the presence of high albedo ice cover is critical to altering the surface energy budget to produce cooling, westerly wind changes, and ventilation. In fact, while *Pausata et al.* [2011] focus on the influence of ice sheet topography in the winter, they show that the summertime meridional temperature gradient is strongly influenced by ice sheet albedo.

3.4. Implications for Paleoclimatic Interpretations

Single-forcing simulations clearly show the reduction of NAM strength in response to LGM boundary conditions, in contrast to some records that suggest a strong LGM NAM [*Lachniet et al.*, 2013]. However, the monsoon is not fully suppressed in our simulations, suggesting that the same fundamental climatological regimes existed in the Southwest during the last glacial period. This coheres with some paleoclimatic evidence that shows the persistence of monsoon-sensitive plant taxa in the NAM region at the LGM [*Holmgren et al.*, 2007]. We also provide a detailed dynamic explanation for the weakening of the NAM at the LGM, which extends previous efforts that hypothesized a role for the westerlies in glacial NAM changes [*Thompson and Anderson*, 2000].

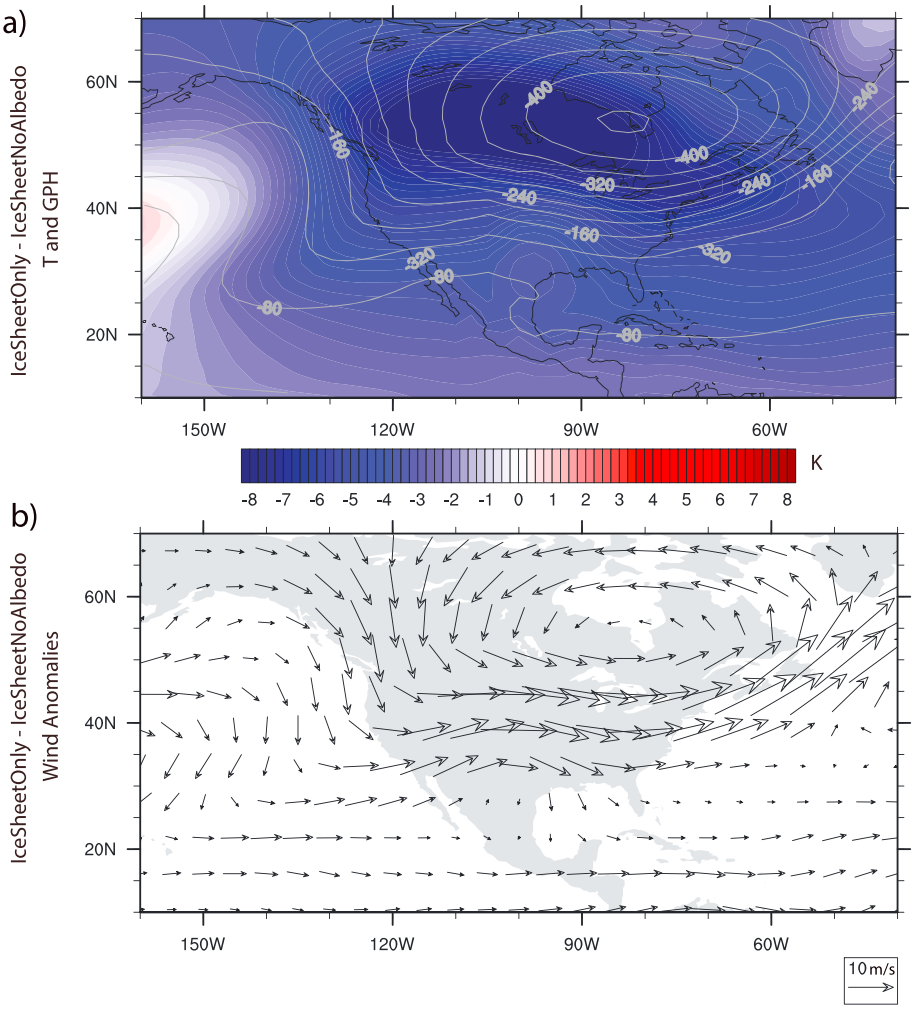

Figure 4. Comparison of CESM runs with ice sheets only (IceSheetOnly) and ice sheets without albedo (IceSheetNoAlbedo), showing (a) stronger 500 hPa meridional temperature gradient in shaded contours and steeper gradient of 500 hPa geopotential height in solid contours, in the simulation that includes high albedo. (b) Shows that this pattern is accompanied by stronger 500 hPa westerly wind anomalies in the IceSheetOnly simulation.

Several paleoclimatic studies suggest a weaker NAM prior to the Holocene, in agreement with our overall observations from model simulations [*Metcalfe et al.*, 2015; *Barron et al.*, 2012; *Antinao and McDonald*, 2013]. However, our interpretation that atmospheric processes play a predominant role in weakening the NAM contrasts with hypotheses that emphasize the role of GoC SSTs. LGM proxy evidence does suggest cooler northeastern Pacific and GoC SSTs [*Lyle et al.*, 2012; *McClymont et al.*, 2012], and our IceSheetOnly simulations produce a similar 4°C of cooling in the GoC as found in proxy records. However, we found that SSTs only play a secondary role in reducing NAM intensity at the LGM, contributing approximately 20% of the rainfall reduction. An interesting consideration is whether strengthening of the NAM across the Pleistocene/Holocene boundary closely tracks GoC SST changes, as previously suggested by *Metcalfe et al.* [2015] and *Barron et al.* [2012] or whether it tracks changes in the latitude of the summertime westerlies, or a combination of these factors. This question could be addressed with detailed proxy records combined with transient climate model simulations spanning this interval.

3.5. Connections Between the NAM, Northern Hemisphere Monsoons, and the Marine ITCZ

Previous studies have argued that NAM strength at the LGM may be linked to changes in the position of the ITCZ [*Lachniet et al.*, 2013; *Jiang et al.*, 2015]. Modeling studies have shown that Northern Hemisphere ice sheets induce an interhemispheric SST gradient and anomalous oceanic heat transports. The ITCZ shifts south as the northern Hadley cell drives a northward cross-equatorial energy transport [*Chiang and Bitz*, 2005]. *McGee et al.* [2014] present LGM proxy evidence of an enhanced interhemispheric SST gradient and estimate

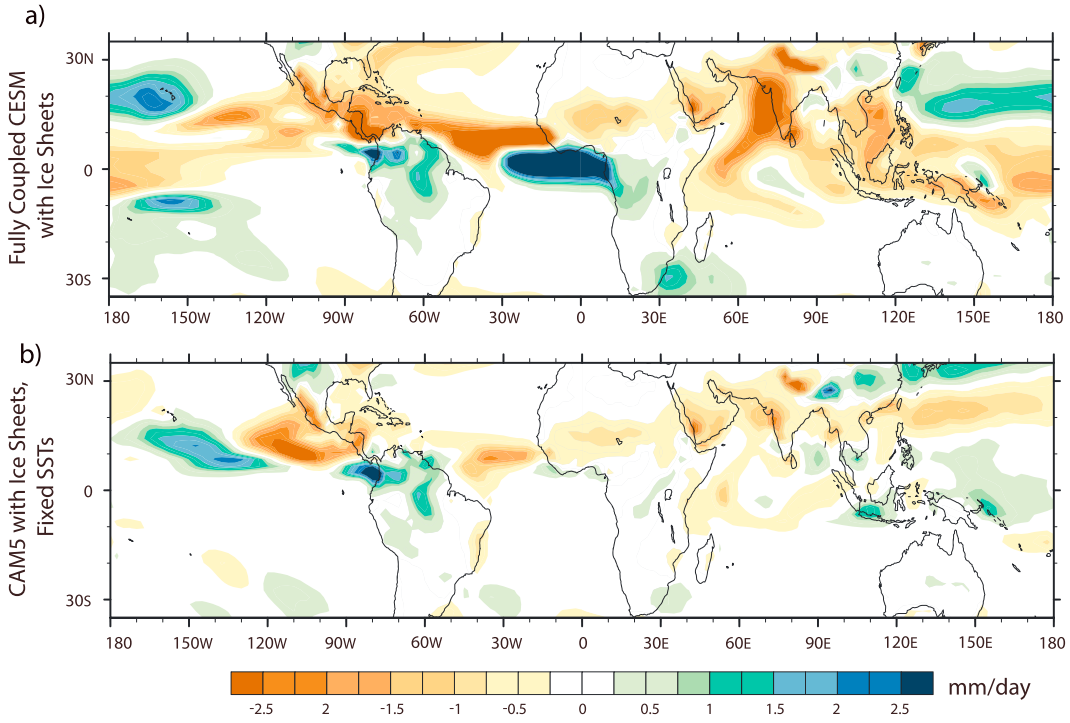

Figure 5. (a) Tropical and monsoon changes in summertime (JAS) rainfall in response to ice sheets in fully coupled CESM with ice sheets (IceSheetOnly), (b) the CAM5 simulation with fixed climatological SSTs (IceSheetAtm). NAM suppression is evident in both simulations, although the marine ITCZ only shifts southward when an interactive ocean is included. Other northern hemisphere monsoons show a weaker response in the atmosphere-only simulation.

a southward shifted ITCZ, supporting this prediction. We suggest that the movement of the marine ITCZ is associated with changes in mean zonal oceanic energy transports, whereas monsoons represent zonally asymmetric extensions of convection over continental areas where *local* changes to the energy budget may be key in determining monsoon convection.

Differences between the tropical precipitation response to ice sheets in the fully coupled model (IceSheetsOnly) and the atmosphere-only model with fixed SSTs (IceSheetAtm) help clarify the distinct influences on the marine ITCZ and the NAM (Figure 5). In the presence of atmosphere-ocean coupling in the full CESM simulation, a southward shift in the marine ITCZ is pronounced, consistent with the mechanism outlined by *Chiang and Bitz* [2005]. CESM1.2 also simulates a reduction in the strength of monsoons in West Africa and South Asia. In the simulation with CAM5 and fixed preindustrial SSTs (IceSheetAtm), there is no ITCZ shift since SSTs do not adjust in response to the ice sheet. Drying in the Asian and West African monsoon regions is also muted, but there is a reduction in the strength of the NAM *equal in magnitude* to the fully coupled simulation (Figure S4). This suggests that atmospheric circulation changes alone contributes more strongly to NAM changes in response to LGM boundary conditions as compared to other monsoon circulations.

We propose two reasons why atmospheric processes may be more important for the glacial response of the NAM in contrast with other monsoon systems. First, in contrast to the South Asian and West African monsoon systems, the NAM is geographically closer to the LGM continental ice sheets, and there are no topographic boundaries that isolate the NAM from the cooling influence of midlatitude circulations. Second, observational evidence of the present-day NAM suggests that moisture advection by the large-scale atmospheric circulation into the core NAM region is a prerequisite to the initiation of the northward surges of moisture that drive NAM convection [*Schiffer and Nesbitt*, 2012]. Given that the climatological state of the NAM features shallower convection and smaller surface MSE values than other monsoon systems (see Figure 1 of *Nie et al.*, 2010], the NAM may be more sensitive to changes in MSE divergence induced by the horizontal flow [*Chou et al.*, 2009]. Our analysis supports this hypothesis by demonstrating the sensitivity of the NAM to LGM changes in the large-scale circulation and showing that the mechanisms that altered the NAM are distinct from those influencing the ITCZ.

4. Conclusions

We used a suite of simulations from CESM1.2 to identify the mechanisms responsible for changes in the North American Monsoon during the LGM. Results suggest that changes in the atmospheric circulation induced by the high albedo of continental ice sheets weaken the NAM. High ice sheet albedo cools the land surface, creating a strong meridional temperature gradient. This weakens the monsoon flow and shifts the westerlies south, creating northwesterly wind anomalies across the NAM region. These wind changes, likely coupled with transient eddy activity, bring cold, dry air into the NAM region. Our emphasis on ice sheet albedo contrasts with previous studies that have found a primary influence of ice sheet topography on the atmospheric circulation. Unlike previous studies, we focus on the summertime circulation, when albedo plays a larger role in the surface energy balance, meridional temperature gradient, and atmospheric response.

While previous research argued that SSTs govern the long-term evolution of the NAM, we suggest that on glacial-interglacial time scales, the atmosphere itself can modulate the strength of the circulation. We show that distinct mechanisms govern the glacial behavior of the ITCZ and the NAM, suggesting that the NAM response to climatic perturbation cannot be predicted by simply understanding ITCZ behavior. In fact, our simulations suggest that the strength of monsoon convection is influenced by the large-scale flow as well as local surface fluxes of heat and moisture [*Chou and Neelin*, 2003; *Privé and Plumb*, 2007]. When considering the future response of the NAM to warming, which may result in a warmer troposphere and higher threshold for convection [see *Chou et al.*, 2009; *Cook and Seager*, 2013], accurately predicting the NAM requires us to understand how local processes and advection might interact to enhance or suppress this unique, regional monsoon.

Acknowledgments
We wish to acknowledge members of NCAR's Climate Modeling Section, CESM Software Engineering Group (CSEG), and Computation and Information Systems Laboratory (CISL) for their contributions to the development of CESM. P.D.N. gratefully acknowledges CGD for supporting a long-term visit to NCAR when these simulations were performed. Funding for the simulations presented here was provided by NSF (grants AGS-1204011 and OCN-1304910). T.B. and J.E.T. acknowledge a David and Lucile Packard Foundation Fellowship in Science and Engineering to J.E.T. as well as NSF grant OCE-1651034. The source code for CESM1.2 is freely available at http://www.cesm.ucar.edu/models/cesm1.2/ following registration. Both the data and input files, as well as model output, will be made available upon request to P.D.N. The data are archived at the University of Texas at Austin Institute for Geophysics. We thank the developers of NCAR's Command Language (NCL), which was used to perform these analyses. We thank the Editor and two reviewers for comments that greatly improved this manuscript.

References

Antinao, J. L., and E. McDonald (2013), An enhanced role for the tropical pacific on the humid Pleistocene-Holocene transition in southwestern North America, *Quat. Sci. Rev.*, *78*, 319–341.

Asmerom, Y., V. J. Polyak, and S. J. Burns (2010), Variable winter moisture in the southwestern United States linked to rapid glacial climate shifts, *Nat. Geosci.*, *3*(2), 114–117.

Barron, J. A., S. E. Metcalfe, and J. A. Addison (2012), Response of the North American Monsoon to regional changes in ocean surface temperature, *Paleoceanography*, *27*, PA3206, doi:10.1029/2011PA002235.

Boos, W. R., and Z. Kuang (2010), Dominant control of the South Asian monsoon by orographic insulation versus plateau heating, *Nature*, *463*(7278), 218–222, doi:10.1038/nature08707.

Bordoni, S., and B. Stevens (2006), Principal component analysis of the summertime winds over the Gulf of California: A gulf surge index, *Mon. Weather Rev.*, *134*(11), 3395–3414.

Braconnot, P., S. P. Harrison, M. Kageyama, P. J. Bartlein, V. Masson-Delmotte, A. Abe-Ouchi, B. Otto-Bliesner, and Y. Zhao (2012), Evaluation of climate models using palaeoclimatic data, *Nat. Clim. Change*, *2*(6), 417–424.

Caballero-Miranda, M. (1997), The last glacial maximum in the Basin of Mexico: The diatom record between 34,000 and 15,000 years B.P. from Lake Chalco, *Quat. Int.*, *43*, 125–136.

Chiang, J. C., and C. M. Bitz (2005), Influence of high latitude ice cover on the marine Intertropical Convergence Zone, *Clim. Dyn.*, *25*(5), 477–496.

Chou, C., and J. D. Neelin (2003), Mechanisms limiting the northward extent of the Northern Summer Monsoons over North America, Asia, and Africa, *J. Clim.*, *16*(3), 406–425.

Chou, C., J. D. Neelin, C.-A. Chen, and J.-Y. Tu (2009), Evaluating the rich-get-richer mechanism in tropical precipitation change under global warming, *J. Clim.*, *22*(8), 1982–2005.

Cook, B., and R. Seager (2013), The response of the North American Monsoon to increased greenhouse gas forcing, *J. Geophys. Res. Atmos.*, *118*, 1690–1699, doi:10.1002/jgrd.50111.

Holmgren, C. A., J. Norris, and J. L. Betancourt (2007), Inferences about winter temperatures and summer rains from the late Quaternary record of C4 perennial grasses and C3 desert shrubs in the northern Chihuahuan Desert, *J. Quat. Sci.*, *22*(2), 141–161.

Holton, J. R., and G. J. Hakim (2012), *An Introduction to Dynamic Meteorology*, vol. 88, Academic Press, New York.

Hurley, J. V., and W. R. Boos (2013), Interannual variability of monsoon precipitation and local subcloud equivalent potential temperature, *J. Clim.*, *26*(23), 9507–9527.

Jiang, D., Z. Tian, X. Lang, M. Kageyama, and G. Ramstein (2015), The concept of global monsoon applied to the last glacial maximum: A multi-model analysis, *Quat. Sci. Rev.*, *126*, 126–139.

Lachniet, M. S., Y. Asmerom, J. P. Bernal, V. J. Polyak, and L. Vazquez-Selem (2013), Orbital pacing and ocean circulation-induced collapses of the Mesoamerican monsoon over the past 22,000 y, *Proc. Natl. Acad. Sci. U.S.A.*, *110*(23), 9255–9260, doi:10.1073/pnas.1222804110.

Lawrence, D. M., et al. (2011), Parameterization improvements and functional and structural advances in Version 4 of the Community Land Model, *J. Adv. Model. Earth Syst.*, *3*, M03001, doi:10.1029/2011MS00045.

Lee, S.-Y., J. C. Chiang, and P. Chang (2015), Tropical pacific response to continental ice sheet topography, *Clim. Dyn.*, *44*(9–10), 2429–2446.

Liu, Y., J. C. Chiang, C. Chou, and C. M. Patricola (2014), Atmospheric teleconnection mechanisms of extratropical North Atlantic SST influence on Sahel rainfall, *Clim. Dyn.*, *43*(9–10), 2797–2811.

Lyle, M., L. Heusser, C. Ravelo, M. Yamamoto, J. Barron, N. S. Diffenbaugh, T. Herbert, and D. Andreasen (2012), Out of the tropics: The Pacific, Great Basin Lakes, and Late Pleistocene water cycle in the western United States, *Science*, *337*(6102), 1629–1633.

Manabe, S., and A. J. Broccoli (1985), The influence of continental ice sheets on the climate of an ice age, *J. Geophys. Res.*, *90*(D1), 2167–2190, doi:10.1029/JD090iD01p02167.

McClymont, E. L., R. S. Ganeshram, L. E. Pichevin, H. M. Talbot, B. E. Dongen, R. C. Thunell, A. M. Haywood, J. S. Singarayer, and P. J. Valdes (2012), Sea-surface temperature records of Termination 1 in the Gulf of California: Challenges for seasonal and interannual analogues of tropical pacific climate change, *Paleoceanography*, *27*, PA2202, doi:10.1029/2011PA002226.

McGee, D., A. Donohoe, J. Marshall, and D. Ferreira (2014), Changes in ITCZ location and cross-equatorial heat transport at the Last Glacial Maximum, Heinrich Stadial 1, and the mid-Holocene, *Earth Planet. Sci. Lett.*, *390*, 69–79.

Metcalfe, S. E., J. A. Barron, and S. J. Davies (2015), The holocene history of the North American Monsoon: Known knowns and known unknowns in understanding its spatial and temporal complexity, *Quat. Sci. Rev.*, *120*, 1–27, doi:10.1016/j.quascirev.2015.04.004.

Meyer, J. D., and J. Jin (2016), The response of future projections of the North American Monsoon when combining dynamical downscaling and bias correction of CCSM4 output, *Clim. Dyn.*, *46*(2961), 1–15, doi:10.1007/s00382-016-3352-8.

Mitchell, D. L., D. Ivanova, R. Rabin, T. J. Brown, and K. Redmond (2002), Gulf of California sea surface temperatures and the North American Monsoon: Mechanistic implications from observations, *J. Clim.*, *15*(17), 2261–2281.

Neale, R. B., et al. (2010), Description of the NCAR Community Atmosphere Model (CAM 5.0), *NCAR Tech. Note NCAR/TN-486+ STR*, Natl. Cent. for Atmos. Res., Boulder, Colo.

Nie, J., W. R. Boos, and Z. Kuang (2010), Observational evaluation of a convective quasi-equilibrium view of monsoons, *J. Clim.*, *23*(16), 4416–4428.

Oster, J. L., D. E. Ibarra, M. J. Winnick, and K. Maher (2015), Steering of westerly storms over western North America at the Last Glacial Maximum, *Nat. Geosci.*, *8*(3), 201–205.

Pausata, F. S. R., C. Li, J. J. Wettstein, M. Kageyama, and K. H. Nisancioglu (2011), The key role of topography in altering North Atlantic atmospheric circulation during the last glacial period, *Clim. Past*, *7*(4), 1089–1101, doi:10.5194/cp-7-1089-2011.

Privé, N. C., and R. A. Plumb (2007), Monsoon dynamics with interactive forcing. Part I: Axisymmetric studies, *J. Atmos. Sci.*, *64*(5), 1417–1430.

Railsback, L. B., G. A. Brook, B. B. Ellwood, F. Liang, H. Cheng, and R. L. Edwards (2015), A record of wet glacial stages and dry interglacial stages over the last 560 kyr from a standing massive stalagmite in Carlsbad Cavern, New Mexico, USA, *Palaeogeogr. Palaeoclimatol. Palaeoecol.*, *438*, 256–266.

Ray, A. J., G. M. Garfin, M. Wilder, M. Vásquez-León, M. Lenart, and A. C. Comrie (2007), Applications of monsoon research: Opportunities to inform decision making and reduce regional vulnerability, *J. Clim.*, *20*(9), 1608–1627.

Roy, P. D., C. M. Chávez-Lara, L. E. Beramendi-Orosco, J. L. Sánchez-Zavala, G. Muthu-Sankar, R. Lozano-Santacruz, J. D. Quiroz-Jimenez, and N. López-Balbiaux (2015), Paleohydrology of the Santiaguillo Basin (Mexico) since late last glacial and climate variation in southern part of western subtropical North America, *Quat. Res.*, *84*(3), 335–347.

Schiffer, N. J., and S. W. Nesbitt (2012), Flow, moisture, and thermodynamic variability associated with Gulf of California surges within the North American Monsoon, *J. Clim.*, *25*(12), 4220–4241.

Schneider, U., A. Becker, P. Finger, A. Meyer-Christoffer, M. Ziese, and B. Rudolf (2014), GPCC's new land surface precipitation climatology based on quality-controlled in situ data and its role in quantifying the global water cycle, *Theor. Appl. Climatol.*, *115*(1–2), 15–40, doi:10.1007/s00704-013-0860-x.

Smith, R., et al. (2010), The Parallel Ocean Program (POP) Reference Manual Ocean Component of the Community Climate System Model (CCSM) and Community Earth System Model (CESM), *Rep. LAUR-01853*, 141 pp.

Thompson, R. S., and K. H. Anderson (2000), Biomes of western North America at 18,000, 6000 and 0 14C yr B.P. reconstructed from pollen and packrat midden data, *J. Biogeogr.*, *27*(3), 555–584, doi:10.1046/j.1365-2699.2000.00427.x.

Turner, R., J. Bowers, and T. Burgess (1995), *Sonoran Desert Plants: An Ecological Atlas*, Univ. of Arizona Press, Tucson, Ariz.

Wagner, J. D., J. E. Cole, J. W. Beck, P. J. Patchett, G. M. Henderson, and H. R. Barnett (2010), Moisture variability in the southwestern United States linked to abrupt glacial climate change, *Nat. Geosci.*, *3*(2), 110–113.